

A NEW SINGULAR PERTURBATION APPROACH FOR IMAGE SEGMENTATION TRACKING

Joël Schaerer² Jérôme Pousin¹ Patrick Clarysse²

¹Institut C. Jordan, CNRS UMR 5028, ²CREATIS-LRMN, CNRS UMR 5220, Inserm U630
INSA of Lyon, 20 av. A Einstein F-69621 Villeurbanne CEDEX France

ABSTRACT

Deformable model based segmentation usually relies on a force field extracted from the image data through the computation of image gradient or gradient vector flow. At convergence, the work of the forces at the interface location should annihilate. This condition is not met in classical deformable formulations. In order to insure this condition, we previously introduced a constrained problem and a nonlinear approach in the framework of a deformable elastic template. From a computational point of view, these two approaches can be very time consuming. Therefore, we propose in this paper a new simpler formulation using a singular perturbation technique. The nice behavior of the proposed model is demonstrated in the context of the segmentation and tracking of the heart contours in 2D cardiac MRI sequences.

Index Terms— Deformable model, singular perturbation method, segmentation tracking, cardiac image sequences

1. INTRODUCTION

Image segmentation is the process that extracts meaningful parts from images for further exploitation and quantification. Still, there is no universal approach to the problem. It is clear however that *a priori* information related to the particular context is needed to particularize any generic segmentation method. Deformable models is a class of methods that has received a lot of attention in the past. They rely on *a priori* reference shape model of the structure to be extracted that is iteratively adapted to the image data. The adaptation process is usually driven by a force field issued from the image through the computation of image gradient or gradient vector flow [1]. In this paper, we consider the segmentation and tracking of soft structures in image sequences. Our applicative context more specifically concerns the extraction of the heart interfaces in Magnetic Resonance Image (MRI) sequences. At convergence, the cumulative force on the contours should approach zero. However, this is not achieved in classical deformable model formulations. To this aim, we

This work has been supported by the Région Rhône-Alpes in the context of project PP3/I3M 'Multiscale Medical Imaging and modeling: from the small animal to the human being' of cluster ISLE.

previously introduced a constrained linear/non linear elastic deformable template [2],[3]. In order to speed up this, sometimes time consuming approach, we propose in this paper a simpler formulation based on a singular perturbation approach which is particularly suited for segmentation tracking in image sequences.

2. METHODS

2.1. The Deformable Elastic Template

Our method is based on the *Deformable Elastic Template* (DET) method introduced by Pham [4],[2] and later improved by Rouchdy [3]. A DET is a combination of :

- A topological and geometric model of the object to be segmented.
- A constitutive equation (elasticity) defining its behavior under applied external image forces that pushes the model's interfaces towards the image edges.

The equilibrium of the model is obtained through the minimization of the following global energy functional :

$$E(v) = E_{elastic}(v) + E_{data}(v)$$

where $E_{elastic}$ represents the deformation energy of the model, E_{data} is the energy due to the external image forces and v is the displacement. Let Ω_0 be the initial configuration of the elastic template, the deformation φ is described by the Green-Lagrange strain tensor which is linearized under the small deformation assumption. We denote by $\epsilon(v) = \frac{1}{2}(\nabla v + \nabla v^T)$ the strain tensor and by $\sigma(v) = \lambda Tr(\epsilon(v))\mathbb{I} + 2\mu\epsilon(v)$ the stress tensor as a function of the displacement v . The coefficients λ and μ stand for the Lamé coefficients (see [5]). The external energy is defined as work produced by the force field \mathbf{f} due to the deformation. We denote by $H^1(\Omega_0)$ the classical Sobolev space of functions in $L^2(\Omega_0)$ with a derivative in distributional sense in $L^2(\Omega_0)$.

$$H^1(\Omega_0) = \{\varphi \in L^2(\Omega_0); D\varphi \in L^2(\Omega_0)\}$$

(see [5]) and we set $\mathbf{H} = (H^1(\Omega_0))^3$.

Let R be the subspace of rigid motions, which is defined as the kernel of the strain tensor: $R = \text{Ker } \epsilon$, set $\mathbb{H} = (H^1(\Omega_0)/R)^3$ the displacement space, equipped with the semi-norm $\|\epsilon(v)\|_{L^2(\Omega_0)}$ which, thanks to the Korn inequality, is a Hilbert space. The following hypotheses for the field \mathbf{f} are convenient for analyzing the asymptotics.

- H1: The function \mathbf{f} is defined on $\mathcal{O} \supset \Omega_0$, and \mathbf{f} is Lipschitz on \mathcal{O} with values in \mathbb{R}^3 . Furthermore, there exists $\mathbf{F} : \mathbb{R}^3 \rightarrow \mathbb{R}^+$ verifying $-D\mathbf{F}(x) = \mathbf{f}(x)$.

The optimality conditions associated to minimizing $E(v)$ on \mathbb{H} read: find the displacement $u \in \mathbb{H}$ verifying:

$$\begin{cases} -\text{div}(\sigma(u)) = 0 & \text{in } \Omega_0; \\ \sigma(I + u) \cdot n = \mathbf{f}(I + u) & \text{on } \partial\Omega_0. \end{cases} \quad (1)$$

Note that $u \neq 0 \Rightarrow \mathbf{f}(I + u) \neq 0$, so forces cannot be null at the solution with this formulation.

2.1.1. The Quasi-Static Lamé System

The problem (1) is nonlinear, thus for computing an approximation with a finite element method, for example ([4]), quasi static or Picard fixed point strategies can be used: find $t \mapsto v(t)$ verifying:

$$\begin{cases} \frac{d}{dt}v(t) - \text{div}(\sigma(v(t))) = 0 & \text{in } \Omega_0 \text{ for } 0 < t; \\ \sigma(I + v(t)) \cdot n = \mathbf{f}(I + v(t)) & \text{on } \partial\Omega_0; \\ v(0) = 0; \end{cases} \quad (2)$$

or, for w^n given, compute w^{n+1} solution to:

$$\begin{cases} -\text{div}(\sigma(w^{n+1})) = 0 & \text{in } \Omega_0; \\ \sigma(I + w^n) \cdot n = \mathbf{f}(I + u) & \text{on } \partial\Omega_0. \end{cases} \quad (3)$$

Then u is defined by $u = \lim_{t \rightarrow \infty} v(t)$; $u = \lim_{n \rightarrow \infty} w^n$.

2.2. Singular Perturbation Technique

Let us introduce a function α satisfying:

- H2: The function $\alpha : \mathbb{R}^+ \rightarrow \mathbb{R}^+$ is regular, integrable over \mathbb{R}^+ , non increasing and bounded from below on any compact subset of \mathbb{R}^+ with $\lim_{t \rightarrow \infty} \alpha(t) = 0$.

We have:

Theorem 1 Assume hypotheses H1 and H2 satisfied. Then for all $0 < t < T$, the following problem

$$\begin{cases} \frac{d}{dt}u(t) - \text{div}(\alpha(t)\sigma(u(t))) = 0 & \text{in } \Omega_0; \\ \alpha(t)\sigma(u(t)) \cdot n = \mathbf{f}(I + u(t)) & \text{on } \partial\Omega_0; \\ u(0) = 0 & \text{in } \Omega_0. \end{cases} \quad (4)$$

has a unique solution $u \in L^2(0, T; ((H^2(\Omega))^3 \cap \mathbb{H}) \cap C^0(0, T; \mathbb{H}))$; $\frac{d}{dt}u \in L^2(0, T; H^2(\Omega_0))^3$

For Problem (4), the asymptotic behavior with respect to time is given in the next theorem.

Theorem 2 Assume hypotheses H1 and H2 satisfied. Then, $u(t)$ solution to (4) converges towards $\bar{u} \in \mathbb{H}$ solution to

$$\mathbf{f}(I + \bar{u}) = 0 \text{ on } \partial\Omega_0. \quad (5)$$

Proof. Let us give a sketch of the proof. Define the bilinear symmetric form $a(\cdot, \cdot)$ associated to the linear elasticity operator by

$$a(v, w) = \alpha(t) \int_{\Omega_0} \mu(\nabla v / \nabla w) + (\lambda + \mu) \text{div}v \text{div}w \, dx.$$

Multiply Equation (4) by $\frac{d}{dt}u$ and integrate over Ω_0 . After some classical calculations, we get:

$$\left\| \frac{d}{dt}u(t) \right\|_{L^2(\omega_0)}^2 + \frac{\alpha(t)}{2} \frac{d}{dt}a(u(t), u(t)) = - \int_{\partial\Omega_0} \frac{d}{dt}\mathbf{F}(u(t)) \, d\xi. \quad (6)$$

For all $0 < t < T$, by integrating by parts the second term, we get:

$$\int_0^t \left\| \frac{d}{ds}u(s) \right\|_{L^2(\omega_0)}^2 \, ds - \int_0^t \frac{\alpha'(s)}{2} a(u(s), u(s)) \, ds + \frac{\alpha(t)}{2} a(u(t), u(t)) + \int_{\partial\Omega_0} \mathbf{F}(u(t)) \, d\xi = \int_{\partial\Omega_0} \mathbf{F}(0) \, d\xi. \quad (7)$$

We deduce the existence of two time-independent constants C_1 and C_2 such that:

$$\left\| \frac{d}{ds}u(s) \right\|_{L^2(0, t; (L^2(\omega_0))^3)} \leq C_1; \quad \|\sqrt{\alpha(t)}u(t)\|_{(H^1(\omega_0))^3} \leq C_2.$$

We conclude that up to a zero measure subset, $\frac{d}{dt}u(t)$ goes to zero when time goes to infinity. Moreover, by considering a variational formulation of Problem (4), we have for all $\varphi \in (H^1(\Omega_0))^3$:

$$\left| \int_{\partial\Omega_0} \mathbf{f}(I + u(t))\varphi \, d\xi \right| \leq \left| \int_{\Omega_0} \frac{d}{dt}u(t)\varphi \, dx \right| + \sqrt{\alpha(t)}a(\sqrt{\alpha(t)}u(t), \varphi). \quad (8)$$

The right hand side of the previous expression goes to zero when t goes to infinity. Since $u(t)$ converges towards \bar{u} and since \mathbf{f} is continuous, we conclude that

$$\lim_{t \rightarrow \infty} \mathbf{f}(I + u(t)) = 0 \text{ on } \partial\Omega_0.$$

□

2.3. Numerical implementation

We implemented the previously described technique using the finite element method for discretizing the spatial functions, and a simple Euler scheme for time integration. In our implementation, we used $\alpha(t) = e^{-\beta t}$. In the finite element formulation, problem (4) becomes:

$$\frac{\mathbf{U}^\lambda - \mathbf{U}^{\lambda-1}}{\Delta\lambda} + e^{-\beta t} \mathbf{K} \mathbf{U}^\lambda = \mathbf{F}(\mathbf{U}^{\lambda-1})$$

or

$$(\Delta\lambda e^{-\beta t} \mathbf{K} + \mathbf{I}) \mathbf{U}^\lambda = \Delta\lambda \mathbf{F}(\mathbf{U}^{\lambda-1}) + \mathbf{U}^{\lambda-1}$$

where \mathbf{F} is the vector of forces sampled at the mesh control points, \mathbf{K} is the stiffness matrix corresponding to the elasticity operator, $\Delta\lambda$ is the integration time step and \mathbf{U} is the displacement vector (displacement of mesh node points). β should be chosen so that the exponential varies slowly compared to $\mathbf{F}(\mathbf{U})$, and thus depends on the lipschitz constant of the force field.

3. EXPERIMENTS ON CARDIAC IMAGE SEQUENCES

In order to test the model on real data, we used the publicly available 4D heart database [6]. This database is composed of cardiac MR images of 18 patients, together with two expert segmentations at end-diastole and end-systole. A short axis slice sequence, corresponding to a median heart level, has been extracted from one patient set.

The initial shape of the model used to extract the left ventricular (LV) contours from the 2D image sequences was simply a ring. Indeed, the shape of a short axis slice of the myocardium in healthy patients is very close to a perfect ring. This ring was meshed with a very simple method : first divide the ring into quadrangles using sectors and concentric rings, then divide each quadrangle into two triangles. Better meshing methods could of course be used, but the triangles generated by our simple method proved good enough for this application.

Since the method ensures that $\mathbf{f}(\mathbf{I} + \mathbf{v}) = \mathbf{0}$ at convergence, we are guaranteed that the contours of the model will match the zeros of the force fields, that is to say, the contours extracted by a low-level preprocessing method. This is very interesting when confidence in these contours is high but can be a problem when they are noisy.

We illustrate the presented method in two cases : first, the classical context of image segmentation using a GVF with a Canny contour map (fig 1 (b)). In this case, the initial contours are quite noisy. The results show that the proposed method can still be used, however, provided that there is good contrast.

Fig 1 (c) shows the results using a very good pre-segmentation step using topological watersheds, as described in [7]. In this case, we have high confidence in the contours and the model is used to estimate motion inside the myocardium rather than only extract contours. In this case, the segmentation is good and the estimated motion is smooth and should be realistic (at least in the radial direction), since the motion is the solution of an elasticity problem and models the myocardium quite well.

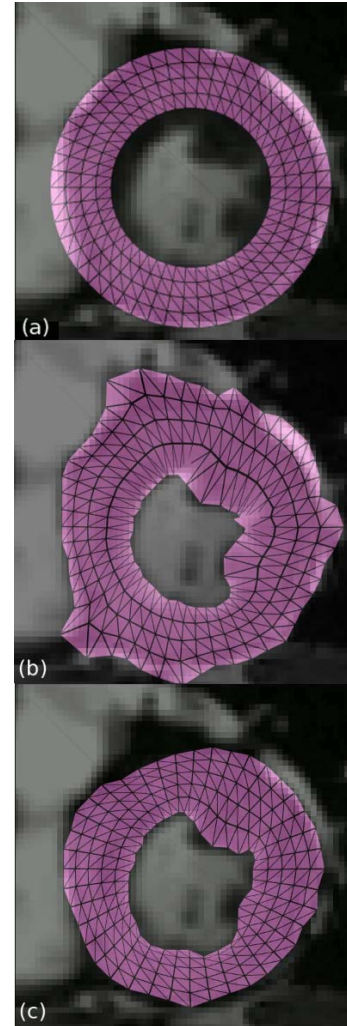


Fig. 1. Result of the constrained deformation of the deformable model on a 2D cardiac MR image slice (mid-systole): (a) initialization, (b) result with GVF force field, (c) result with morphological pre-segmentation

The singular perturbative method introduced in this paper can be applied straightforwardly to the dynamic elastic model introduced in [8]. Fig 2 shows the results of the constrained dynamic model on the whole cardiac sequence, for the same 2D slice shown in Fig 1, using the watershed contour extraction described above.

Computation times using the singular perturbation technique are similar to what is observed with the normal Deformable Elastic Template: less than a minute is needed to analyze a 2D+t MRI sequence on a standard PC with a Python language implementation of the model.

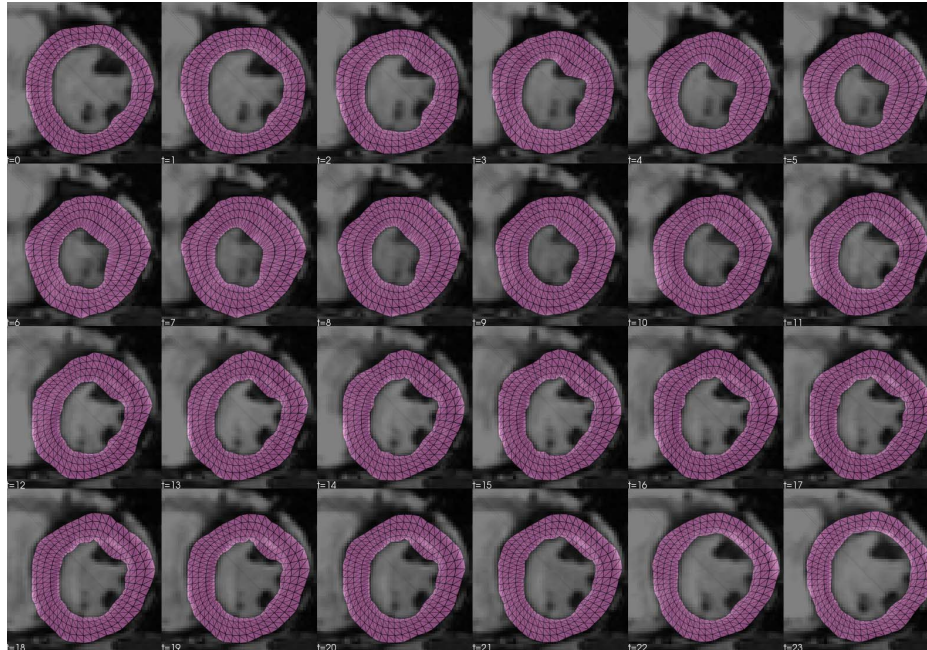


Fig. 2. Results on a dynamic sequence. $t=0$ corresponds to end-diastole.

4. CONCLUSIONS AND PERSPECTIVES

We have presented a novel algorithm for the constrained segmentation problem with the DET. This algorithm is proved to converge towards a solution of the continuous problem (1) and to impose the condition $f(\mathbf{I} + \mathbf{v}) = \mathbf{0}$. It is to our knowledge the first one to yield an elastic solution while imposing this condition. Such a constraint is particularly useful when the force field is of good quality, and extends the domain of application of the DET.

5. REFERENCES

- [1] Chenyang Xu and Jerry L. Prince, "Snakes, shapes, and gradient vector flow," *IEEE Transactions on Image Processing*, vol. 7, pp. 359–369, 1998.
- [2] T. Mäkelä, Q.-C. Pham, P. Clarysse, J. Nenonen, J. Lötjönen, O. Sipilä, H. Hänninen, K. Lauerma, J. Knuuti, T. Katila, and I. E. Magnin, "A 3-D model-based registration approach for the PET, MR and MCG cardiac data fusion," *Medical Image Analysis*, vol. 7, pp. 377–389, 2003.
- [3] Y. Rouchdy, J. Pousin, J. Schaefer, and P. Clarysse, "A nonlinear elastic deformable template for soft structure segmentation. Application to the heart segmentation in MRI," *Inverse Problems*, 2007.
- [4] Q.C. Pham, F. Vincent, P. Clarysse, P. Croisille, and I.E. Magnin, "A FEM-based deformable model for the 3D segmentation and tracking of the heart in cardiac MRI," in *Proceedings of the 2nd International Symposium on Image and Signal Processing and Analysis (ISPA 2001)*, 2001, pp. 250–254.
- [5] P. G. Ciarlet, *Mathematical Elasticity Volume I: Three-Dimensional Elasticity*, North-Holland, Amsterdam, 1988.
- [6] L. Najman, J. Cousty, M. Couprie, H. Talbot, S. Clément-Guinaudeau, T. Goissen, and J. Garot, "An open, clinically-validated database of 3D+t cine-MR images of the left ventricle with associated manual and automated segmentation," *Insight Journal*, 2007.
- [7] J. Cousty, L. Najman, M. Couprie, S. Clément-Guinaudeau, T. Goissen, and J. Garot, "Automated, accurate and fast segmentation of 4D cardiac MR images," in *Functional Imaging and Modeling of the Heart*, 2007, vol. LNCS 4466, pp. 474–483.
- [8] J. Schaefer, P. Clarysse, and J. Pousin, "A New Dynamic Elastic Model for Cardiac Image Analysis," in *Proceedings of the 29th Annual International Conference of the IEEE EMBS*, Lyon, France, Aug. 2007, pp. 4488–4491.